Int. J. Heat Mass Transfer. Vol. 16, pp 1877–1888 Pergamon Press 1973. Printed in Great Britain

FILM BOILING OF SATURATED BINARY MIXTURES

P.-L. YUE* and M. E. WEBER
Department of Chemical Engineering, McGill University, Montreal, Quebec, Canada

(*Received* 27 *July* 1971 *and in revised form* 22 *January* 1973)

Abstract—Stable film boiling of a saturated binary mixture is analyzed by the two-phase boundary layer theory. Both diffusion and heat conduction in the liquid phase are taken into account. The analysis shows that large increases in film boiling heat flux may be obtained for mixtures with large relative volatility. The increased heat transfer is shown to occur only at small values of the wall superheat. Experiments on a $\frac{5}{16}$ in. dia horizontal cylinder in a number of organic mixtures at atmospheric pressure showed good agreement with the theory.

NOMENCLATURE

C, dimensionless quantity, equations (27) and (31);
c_p, specific heat;
D, diameter of cylinder;
$\mathscr{D}$, diffusivity;
f, dimensionless velocity function, equations (28) and (32);
g, acceleration due to gravity;
g_c, gravitational conversion factor;
Gr, Grashof number, equation (57);
Gr_d, Grashof number in the case of cylinder, equation (60);
Δh, latent heat of vaporization;
k, thermal conductivity;
L, height of vertical plate;
$\dot{m}$, mass flux;
$\overline{Nu}$, average Nusselt number for a plate, equation (56);
$\overline{Nu}_d$, average Nusselt number for a cylinder, equation (59);
Pr, Prandtl number;
$\bar{q}$, average heat flux;
R, $\rho\mu$ ratio, equation (61);
Sc_L, Schmidt number of liquid;
Sp, dimensionless degree of superheating, equation (64);
T, temperature;
ΔT, temperature drop;
u, velocity component in y-direction;
v, velocity component in z-direction;
V, dimensionless quantity, equation (62);
x, weight fraction of component 1 in liquid;
x^*, weight fraction of component 1 in vapor at equilibrium.

Greek symbols

α, thermal diffusivity;
α_{12}, relative volatility;
β, coefficient of volumetric expansion;
δ, boundary layer thickness;
η, similarity variable, equations (26) and (30);
θ, dimensionless temperature, equations (29) and (33);
μ, viscosity;
ν, kinematic viscosity;
ξ, dimensionless concentration, equation (34);
ρ, density;
ψ, stream function, equations (24) and (25).

* Present address: School of Chemistry and Chemical Engineering, The University of Bath, Bath, England.

Subscripts

V, vapor;
L, liquid;
w, heating surface;
i, the vapor–liquid interface;
∞, in the liquid far from the heating surface;
1, component 1;
2, component 2;
min, minimum stable film boiling.

INTRODUCTION

SATURATED film boiling was first successfully analyzed by Bromley [1]. The analysis was based on the assumption that the inertial terms of the equation of motion for the vapor film are negligibly small and that the temperature profile across the vapor film is linear. The velocity at the vapor–liquid interface was taken as zero. Later workers employed the concept of a two-phase boundary layer. The vapor film was treated as a boundary layer. The ascent of vapor induced upward movement of the liquid close to the interface. This liquid film also behaved as a boundary layer. Koh [2] considered saturated film boiling from a vertical plate in terms of the boundary layer equations for the vapor and the liquid. The inertial terms were retained in the equations of motion for the two phases. At the interface, the tangential velocities and shearing stresses of the vapor and the liquid were considered equal. The interfacial temperature was the saturation temperature. Sparrow and Cess [3] examined the effects of subcooling. The vapor–liquid interface was assumed to be stationary. Since the temperature of the liquid bulk was below the saturation temperature, the energy equation for the liquid entered the analysis. The interface was taken to be at saturation. Nishikawa and Ito [4] removed the assumption of a stationary interface by adopting the interfacial conditions of Koh [2].

Experimental film boiling data for mixtures do not agree with these theories. Dunskus and Westwater [5] found that traces of high molecular weight non-volatile additives increased heat transfer to isopropanol in film boiling. Kautzky and Westwater [6] also obtained anomalous results with a miscible mixture of volatile liquids in film boiling on a horizontal plate.

The present work analyses film boiling of saturated binary mixtures. A two-phase boundary layer theory for binary mixtures is formulated to examine the role of mass diffusion in the heat transfer process. The predictions of the theory are compared with experimental data taken on a horizontal cylinder with organic mixtures.

ANALYSIS

The analysis is presented for the vertical plate and then the transformation of Nishikawa and Ito [4] is used for the horizontal cylinder.

Vertical plate

The physical model assumes a continuous vapor film over the surface. Adjacent to the vapor film is the liquid boundary layer. Far from the vapor–liquid interface the liquid composition is x_∞ and the temperature is T_∞, the saturation temperature. Due to evaporation and diffusion the liquid composition x_i at the vapor–liquid interface is not that of the bulk. If vapor–liquid equilibrium is assumed, the interfacial temperature T_i is dictated by x_i and the total pressure. T_i is higher than T_∞, but its actual value is unknown *a priori*. The vapor at the interface has a composition x_i^* which is also determined by the thermodynamic equilibrium data for the mixture. The geometry is shown in Fig 1.

Basic equations

The conservation equations for mass, momentum and energy for steady laminar flow in the vapor boundary layer on a vertical plate are [9]:

$$\text{Continuity} \quad \frac{\partial u_V}{\partial y} + \frac{\partial v_V}{\partial z} = 0 \tag{1}$$

$$\text{Momentum} \quad u_V \frac{\partial u_V}{\partial y} + v_V \frac{\partial u_V}{\partial z} = \frac{g(\rho_L - \rho_V)}{\rho_V} + \nu_V \frac{\partial^2 u_V}{\partial z^2} \tag{2}$$

Energy $$u_V \frac{\partial T_V}{\partial y} + v_V \frac{\partial T_V}{\partial z} = \alpha_V \frac{\partial^2 T_V}{\partial v^2}. \quad (3)$$

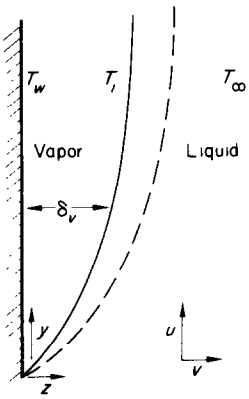

FIG. 1. Physical model for vertical plate.

Assuming that diffusion in the vapor has a minor effect on heat transfer, the diffusion equation for the vapor phase was omitted. This simplification makes it possible to obtain similarity transformations for the differential equations. The same simplification was used by Koh [8] in his analysis of binary film condensation.

For the liquid boundary layer the buoyancy term in the momentum equation is expressed in the free convection form and the diffusion equation is included:

Continuity $$\frac{\partial u_L}{\partial y} + \frac{\partial v_L}{\partial z} = 0 \quad (4)$$

Momentum $$u_L \frac{\partial u_L}{\partial y} + v_L \frac{\partial u_L}{\partial z} = g\beta_L(T_L - T_\infty) + \nu_L \frac{\partial^2 u_L}{\partial z^2} \quad (5)$$

Energy $$u_L \frac{\partial T_L}{\partial y} + v_L \frac{\partial T_L}{\partial z} = \alpha_L \frac{\partial^2 T_L}{\partial z^2} \quad (6)$$

Diffusion $$u_L \frac{\partial x}{\partial y} + v_L \frac{\partial x}{\partial z} = \mathscr{D}_L \frac{\partial^2 x}{\partial z^2}. \quad (7)$$

The fluid properties in the boundary layers are considered constant and are evaluated at the mean film temperature of the vapor or the liquid accordingly.

Boundary and interface conditions

At $z = 0$ $$u_V = 0 \quad (8)$$

$$v_V = 0 \quad (9)$$

$$T_V = T_w. \quad (10)$$

At $z \to \infty$ $$u_L = 0 \quad (11)$$

$$x = x_\infty \quad (12)$$

$$T = T_\infty. \quad (13)$$

At $z = \delta_V^+$ $$x = x_i \quad (14)$$

$z = \delta_V^-$ $$x = x_i^* \quad (15)$$

$$T = T_i(x_i). \quad (16)$$

Since the liquid velocity tangent to the interface is the same as that of the vapor:

at $z = \delta_V$ $$(u_V)_i = (u_L)_i. \quad (17)$$

Since the mass transfer across the interface is continuous:

at $z = \delta_V$ $$\rho_V\left(v_V - u_V \frac{\mathrm{d}\delta}{\mathrm{d}y}\right)_i = \rho_L\left(v_L - u_L \frac{\mathrm{d}\delta}{\mathrm{d}y}\right)_i. \quad (18)$$

Assuming that the tangential shearing stress at the interface is the same for both the vapor and the liquid:

at $z = \delta_V$ $$\mu_V\left(\frac{\partial u_V}{\partial z}\right)_i = \mu_L\left(\frac{\partial u_L}{\partial z}\right)_i. \quad (19)$$

An energy balance at the interface yields:

$$-k_V\left(\frac{\partial T_V}{\partial z}\right)_i = -\rho_V\left(v_V - u_V \frac{\mathrm{d}\delta}{\mathrm{d}y}\right)_i \Delta h - k_L\left(\frac{\partial T_L}{\partial z}\right)_i. \quad (20)$$

Mass balances at the interface yield:

$$(\dot{m}_1)_i = -\rho_L \mathscr{D}_L\left(\frac{\partial x}{\partial z}\right)_i + \frac{\rho_1}{\rho_L}(\dot{m}_1 + \dot{m}_2)_{L,i} \quad (21)$$

$$(\dot{m}_2)_i = \rho_L \mathscr{D}_L \left(\frac{\partial x}{\partial z}\right)_i + \frac{\rho_2}{\rho_L}(\dot{m}_1 + \dot{m}_2)_{L,i}. \quad (22)$$

The vapor-side composition is

$$x_i^* = \frac{(\dot{m}_1)_i}{(\dot{m}_1)_i + (\dot{m}_2)_i}. \quad (23)$$

Similarity transformation

The continuity equation is satisfied by introducing the stream functions ψ_V and ψ_L, such that

$$u_V = \frac{\partial \psi_V}{\partial z} \qquad v_V = -\frac{\partial \psi_V}{\partial y} \quad (24)$$

$$u_L = \frac{\partial \psi_L}{\partial z} \qquad v_L = -\frac{\partial \psi_L}{\partial y}. \quad (25)$$

The partial differential equations are transformed to ordinary differential equations through the following similarity transformation:

Vapor

$$\eta_V = C_V z y^{-\frac{1}{4}} \quad (26)$$

$$C_V = \left[\frac{g(\rho_L - \rho_V)}{4\nu_V^2 \rho_V}\right]^{\frac{1}{4}} \quad (27)$$

$$f_V(\eta_V) = \frac{\psi_V}{4 C_V \nu_V y^{\frac{3}{4}}} \quad (28)$$

$$\theta_V(\eta_V) = \frac{T_V - T_\infty}{T_w - T_\infty} \quad (29)$$

Liquid

$$\eta_L = C_L z y^{-\frac{1}{4}} \quad (30)$$

$$C_L = \left[\frac{g\beta_L(T_w - T_\infty)}{4\nu_L^2}\right]^{\frac{1}{4}} \quad (31)$$

$$f_L(\eta_L) = \frac{\psi_L}{4 C_L \nu_L y^{\frac{3}{4}}} \quad (32)$$

$$\theta_L(\eta_L) = \frac{T_L - T_\infty}{T_w - T_\infty} \quad (33)$$

$$\xi_L(\eta_L) = \frac{x}{x_\infty}. \quad (34)$$

The transformed equations are:

Vapor

Momentum $$f''' + 3 f_V f_V' - 2(f_V')^2 + 1 = 0 \quad (35)$$

Energy $$\theta_V'' + 3 Pr_V f_V \theta_V' = 0 \quad (36)$$

Liquid

Momentum $$f_L''' + 3 f_L f_L'' - 2(f_L')^2 + \theta_L = 0 \quad (37)$$

Energy $$\theta_L'' + 3 Pr_L f_L \theta_L' = 0 \quad (38)$$

Diffusion $$\xi_L'' + 3 Sc_L f_L \xi_L' = 0. \quad (39)$$

The boundary conditions are:

at $\eta_V = 0$

$$f_V = 0 \quad (40)$$

$$f_V' = 0 \quad (41)$$

$$\theta_V = 1 \quad (42)$$

at $\eta_L \to \infty$

$$f_L = 0 \quad (43)$$

$$\theta_L = 0 \quad (44)$$

$$\xi_L = 1. \quad (45)$$

The interface conditions are:

at $\eta_V = \eta_L = \eta_i$

$$(\theta_V)_i = (\theta_L)_i = \frac{T_i - T_\infty}{T_w - T_\infty} \quad (46)$$

$$(\xi_L)_i = \frac{x_i}{x_\infty}.$$

Equations (17)–(20) and (22) become

$$(f_L')_i = B \cdot (f_V')_i \quad (47)$$

where

$$B = [\beta_L(T_w - T_\infty)]^{-\frac{1}{2}} \left[\frac{\rho_V}{\rho_L}\right]^{-\frac{1}{2}} \quad (48)$$

$$(f_L)_i = A \cdot (f_V)_i \quad (49)$$

where

$$A = [\beta_L(T_w - T_\infty)]^{-\frac{1}{4}} \left[\frac{\mu_V}{\mu_L}\right]^{\frac{1}{4}} \left[\frac{\rho_V}{\rho_L}\right]^{\frac{1}{4}} \quad (50)$$

$$(f_L'')_i = A \cdot B (f_V'')_i \quad (51)$$

$$\frac{c_{pV}(T_w - T_\infty)}{\Delta h Pr_V} = -3\frac{(f_V)_i}{(\theta'_V)_i} + D\frac{(\theta'_L)_i}{(\theta'_V)_i} \quad (52)$$

where

$$D = \left(\frac{k_V}{k_L}\right)^{-1}\left(\frac{\mu_V}{\mu_L}\right)^{\frac{1}{4}}\left(\frac{\rho_V}{\rho_L}\right)^{-\frac{1}{4}} \times [\beta_L(T_w - T_\infty)]^{\frac{1}{4}}\left[\frac{c_{pV}}{\Delta h Pr_V \beta_L}\right] \quad (53)$$

$$\frac{x_i^* - x_i}{x_\infty} = \frac{1}{3Sc_L}\frac{(\xi'_L)_i}{(f_L)_i}. \quad (54)$$

Heat transfer

The average heat transfer rate is expressed in terms of dimensionless quantities as

$$\tfrac{3}{4}\overline{Nu}(Gr/4)^{-\frac{1}{4}} = -(\theta'_V)_w \quad (55)$$

where

$$\overline{Nu} = \frac{\bar{q}L}{k_V(T_w - T_\infty)} \quad (56)$$

$$Gr = \frac{g(\rho_L - \rho_V)L^3}{\nu_V^2 \rho_V}. \quad (57)$$

Horizontal cylinder

Nishikawa and Ito [4] have shown that by choosing the appropriate similarity variables equations (35)–(54) also apply to the horizontal cylinder. The final expression for the average Nusselt number for a cylinder is:

$$\frac{1}{0{\cdot}728}(\overline{Nu_d})(Gr_d)^{-\frac{1}{4}} = -(\theta'_V)_w \quad (58)$$

where

$$\overline{Nu_d} = \frac{\bar{q}D}{k_V(T_w - T_\infty)} \quad (59)$$

$$Gr_d = \frac{g(\rho_L - \rho_V)D^3}{\nu_V^2 \rho_V}. \quad (60)$$

Thus, the solution for the vertical flat plate can also be used for the horizontal cylinder.

Equations (35)–(54) were solved numerically. Since the interfacial conditions were not known, a trial-and-error approach was required. For chosen values of (η_V) and $(\eta_L)_i$ the conservation equations for the two phases were solved simultaneously by successive approximation. A finite difference method with an accuracy in the order of $(\Delta\eta)^2$ was used. Details may be found in [7].

THEORETICAL RESULTS AND DISCUSSION

The following set of eight parameters is needed to specify the solution of the system of equations.

$$R, V, \hat{C}_p, Sp, Pr_V, Pr_L, Sc_L, \alpha_{12}.$$

The first four parameters arise from the interfacial conditions.

$$R = \left[\frac{(\rho\mu)_V}{(\rho\mu)_L}\right]^{\frac{1}{4}} \quad (61)$$

$$V = R\left(\frac{\rho_V}{\rho_L}\right)^{-\frac{1}{4}}\left[\frac{c_{pV}}{\beta_L Pr_V \Delta h}\right]^{\frac{1}{4}} \quad (62)$$

$$\hat{C}_p = \frac{c_{pV}}{c_{pL}} \quad (63)$$

$$Sp = \frac{c_{pV}(T_w - T_\infty)}{Pr_V \Delta h}. \quad (64)$$

R is the $\rho\mu$ ratio which is often used in the theory of the two-phase boundary layer [2–4]. The dimensionless number V is similar to the one used in [3] and [4] (defined as R in [3]). Sp is a dimensionless temperature difference. In terms of these parameters, A, B and D used in the interfacial conditions (47), (49) and (52) are:

$$A = V(Sp)^{-\frac{1}{4}} \quad (65)$$

$$B = \left(\frac{V}{R}\right)^2 (Sp)^{-\frac{1}{4}} \quad (66)$$

$$D = \left(\frac{Pr_V}{Pr_L}\right)\frac{Sp^{\frac{1}{4}}}{\hat{C}_p V}. \quad (67)$$

The last two of the eight parameters appear because of the binary mixture.

Velocity, temperature and concentration profiles

The transformed variables f'_V and f'_L may be

taken as velocity distributions of the vapor and the liquid boundary layers, respectively. Figure 2 shows typical velocity profiles for two film thicknesses. Since the value of B in equation (47) is not necessarily unity, there is a discontinuity in f' at the interface. The vapor velocity profile exhibits a maximum which increases with the thickness of the vapor film. The velocity profiles are similar to those of Koh [2] for saturated film boiling.

Figure 3 shows the temperature profiles which correspond to the velocity profiles of Fig. 2. For

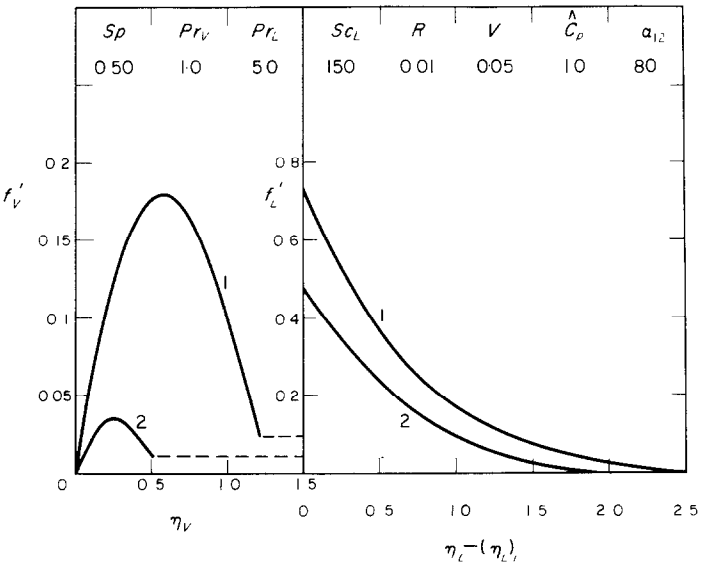

FIG. 2. Velocity profiles in vapor and liquid.

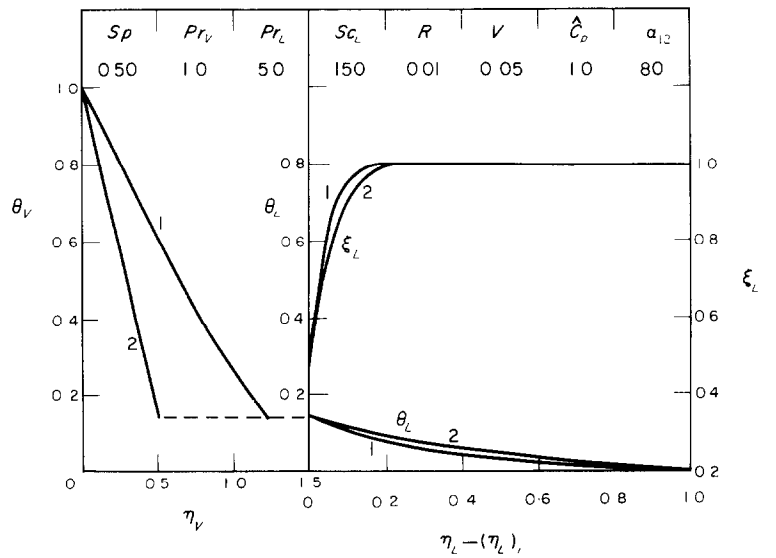

FIG. 3. Temperature profiles in vapor and liquid and concentration profiles in liquid.

thin vapor films the temperature profile is nearly linear. As the vapor film thickens, the profile becomes curved. The shape of the liquid temperature profile is not sensitive to the vapor film thickness. For mixtures with low relative volatility the temperature at the vapor–liquid interface is close to the bulk saturation temperature while for mixtures with high relative volatility the vapor–liquid interface temperature is above the bulk saturation temperature. The concentration profiles in the liquid boundary layer are also shown in Fig. 3. For mixtures with high relative volatility, the concentration at the interface is appreciably less than the bulk concentration. The concentration boundary layer is only one-quarter to one-fifth as thick as the temperature boundary layer because of the high Schmidt number.

Heat transfer results

Figures 4–7 present the dimensionless heat transfer rates as a function of Sp. The ordinate in these figures is $\frac{1}{0{\cdot}728}\overline{Nu}_d(Gr_d/4)^{-\frac{1}{4}}$. the dimensionless heat transfer parameter for horizontal cylinders. It is equivalent to $\frac{3}{4}\overline{Nu}(Gr/4)^{-\frac{1}{4}}$ which is the appropriate dimensionless variable for the vertical plate.

Figure 4 shows that high relative volatility increases heat transfer at low superheat. At higher superheats the influence of relative volatility decreases and eventually becomes negligible at very high superheats ($Sp > 3$). This behavior is due to heat conduction into the liquid away from the vapor–liquid interface. The rate of heat conduction to the liquid is limited by a maximum temperature difference between the vapor–liquid interface and the bulk of the liquid. This maximum occurs when the liquid at the interface contains only the less volatile component. The maximum temperature difference can be approached for mixtures with high α_{12}. However, even in this case as Sp is increased the amount of heat conducted into the liquid reaches its maximum value and thus it becomes a decreasing fraction of the total heat flux.

Figure 5 shows that R has an important effect; the larger R the greater the heat transfer. The resistance to the movement of the liquid boundary layer is less at high R, i.e. when the density or the viscosity of the liquid is lower. This reduction in the resistance to the liquid movement results in an increase in heat transfer. This is in accord with the results of Koh [2].

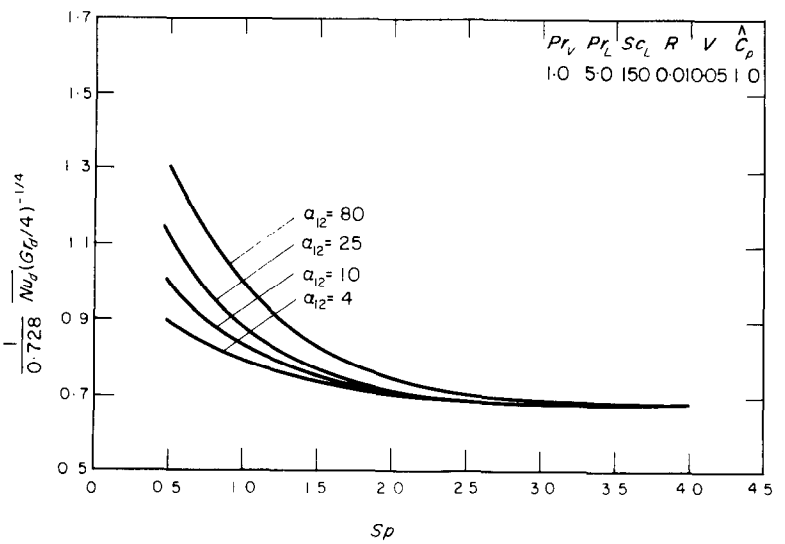

FIG. 4. Effect of relative volatility on heat transfer.

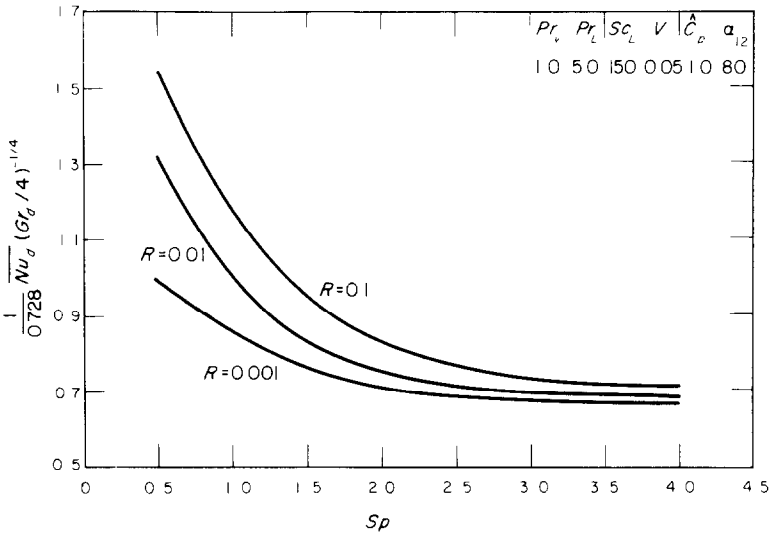

FIG. 5. Effect of R on heat transfer.

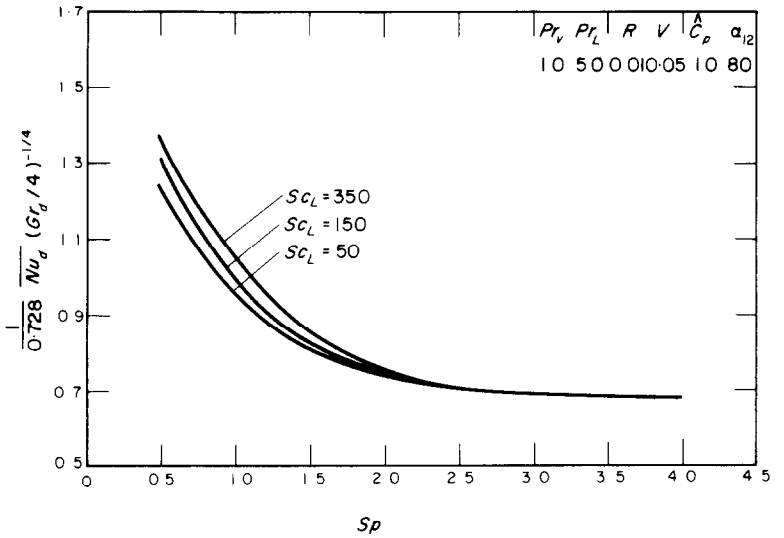

FIG. 6. Effect of liquid Schmidt number on heat transfer.

The Schmidt number of the liquid affects diffusion in the liquid and the concentration at the interface. It is shown in Fig. 6 that higher Schmidt numbers increase heat transfer at values of Sp less than about two. High Schmidt numbers produce lower diffusion rates in the liquid thus yielding lower weight fraction of the more volatile component at the vapor–liquid interface. This raises the interface temperature and increases conduction heat transfer in the liquid. At higher superheat the effect of diffusion on heat transfer becomes negligible as noted above.

The remaining variables have only a minor

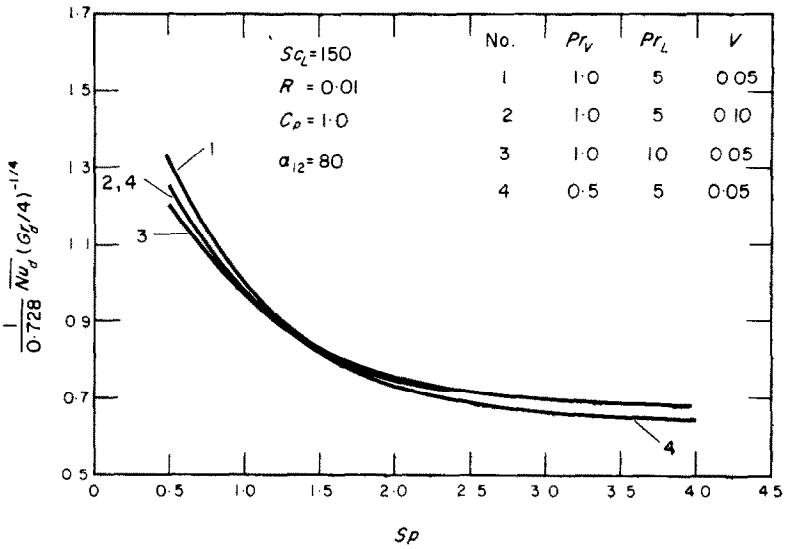

FIG. 7. Effect of Prandtl number and V on heat transfer.

effect on heat transfer. Figure 7 shows that even at low Sp the effect of Pr_V, Pr_L and V is small. At low Sp increasing liquid Prandtl number increases shear stress at the vapor–liquid interface, thus reducing heat transfer.

EXPERIMENTAL STUDY

Film boiling was studied on a horizontal carbon cylinder. The apparatus consisted of a carbon tube heating element housed in a brass boiling chamber. The tube was made of pressed graphite and carbon; 6 in. long, $\frac{5}{16}$ in, o.d. and $\frac{5}{32}$ in. i.d. The middle 3 in. of the tube was the test section in the experiments. A spring assembly was used to keep the tube under compression for good electrical contact.

The nucleate boiling region at the connectors to the carbon tube was prevented from spreading across the tube by cutting two grooves near the ends of the tube. A number of configurations were tried with $\frac{1}{2}$ in. wide by 0·04 in. deep grooves giving the lowest values for $\bar{q}_{min}$ and ΔT_{min}. Most of the data were taken near the minimum film boiling heat flux since the theory indicated that mixture effects were the most significant at low wall superheat.

The boiling chamber had front and rear windows for viewing and photographic measurements. The chamber was filled through a valve at the bottom. Vapor was led off through a tube into a reflux condenser where the condensate could be drawn off for composition measurements or recycled to the boiling chamber. The condensate flow rate was measured for heat balance checks.

A 0·001Ω precision resistor connected in series with the heating element was used for determining the current. Voltages across the test section of the carbon tube and the precision resistor were measured by an integrating digital voltmeter.

The temperature of the inside of the carbon tube was measured by a chromel–alumel thermocouple which was coated with a thin layer of porcelain cement. The surface temperature of the tube was calculated. Compositions of liquid and vapor mixtures were determined by refractive index measurements. Details of the experi-

mental apparatus and procedure can be found in [7].

Experimental results and discussion

Photographs of the boiling process showed that vapor bubbles were released only at the top of the tube. The vapor film was fairly smooth except at the top where the bubbles were released. The two-phase boundary layer model was a realistic description of film boiling in mixtures and pure components on a cylinder of the size used here.

In Figs. 8–10 the experimental data are compared with theoretical predictions. The predicted values were obtained by using physical properties appropriate to the mixture under study. Details are reported in [7]. In calculating the theoretical values, radiant heat transfer was included by adding the radiant flux to that calculated from the two-phase boundary layer analysis, assuming a nonparticipating vapor as discussed by Sparrow [10]. An additional complication is involved here beyond the film thickening shown by Sparrow. For a mixture the radiant flux vaporizes some liquid, thus affecting the diffusion in the liquid phase and the vapor–liquid interface temperature and composition. A complete treatment would be very complex. Since radiation contributes only about 10–15 per cent of the total flux at the low temperature levels of this study, the simple addition of fluxes is adequate.

Figures 8 and 9 show experimental heat fluxes as a function of composition at constant values of ΔT, the heater to bulk liquid temperature difference. It is seen in Fig. 8 that $\bar{q}$ is nearly constant with composition for n-hexane/toluene mixtures. The relative volatility of this mixture is about 4. The experimental results are in good agreement with the two-phase boundary layer theory. Bromley's theory also is adequate for evaluating $\bar{q}$ for the entire range of composition. The two-phase boundary layer theory also gave a good fit to data for systems with azeotropes. An example is the ethanol/benzene mixture also shown in Fig. 8. This pair has an azeotrope at

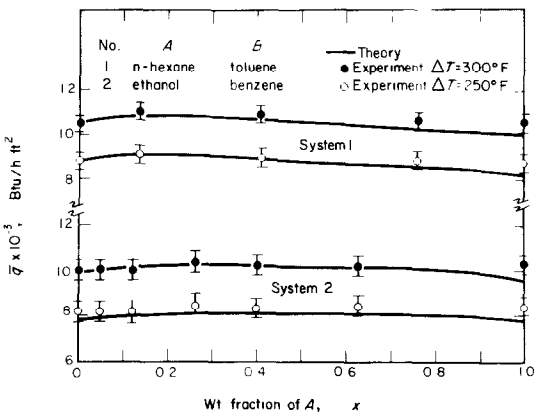

FIG. 8. Effect of composition on heat flux at constant temperature for two systems.

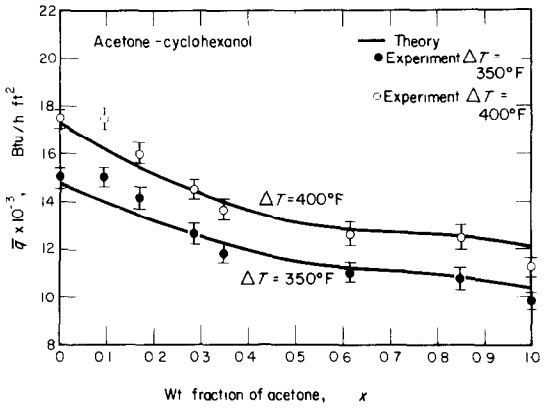

FIG. 9. Effect of composition on heat flux at constant temperature difference for acetone–cyclohexanol.

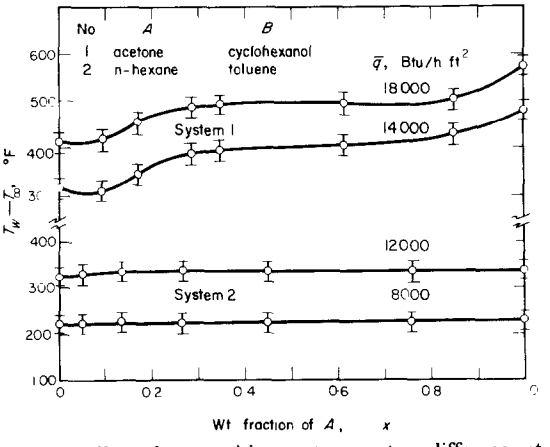

FIG. 10. Effect of composition on temperature difference at constant heat flux for two systems.

32·5 per cent (by weight) ethanol. There was no unusual behavior near the azeotropic composition. This is in marked contrast to the behavior in nucleate boiling of the same mixture [11].

In the case of systems with high relative volatility, such as the acetone/cyclohexanol mixtures ($\alpha_{12} \approx 80$), the predictions are in good agreement with the data as shown in Fig. 9. For this mixture Bromley's simple relation yields fluxes that are up to 30 per cent too low.

The variation of the temperature difference with composition at constant heat flux for two systems is shown in Fig. 10. The change in ΔT in acetone/cyclohexanol mixtures is much greater than that in other mixtures and is accurately predicted by the theory.

A number of other mixtures were also tested with results in accord with the theory as shown here. Details can be found in [7].

CONCLUSIONS

Saturated film boiling of binary mixtures has been successfully analyzed by the two-phase boundary layer theory including diffusion in the liquid. For mixtures the temperature at the vapor–liquid interface is greater than the saturation temperature of the mixture. As a result heat is conducted into the liquid and mixtures with high relative volatilities give heat fluxes higher than those predicted by Bromley's theory which accounts only for vaporization. This effect is most significant for mixtures with high relative volatility at low wall superheat.

Experimental film boiling fluxes measured on a horizontal cylinder agreed well with the theory. For mixtures with relative volatilities lower than about 4, Bromley's theory is adequate. For mixtures with higher relative volatilities the theory presented here should be used.

ACKNOWLEDGEMENT

This work was supported by the National Research Council of Canada.

REFERENCES

1. L. A. Bromley, Heat transfer in stable film boiling, *Chem. Engng Prog.* **46**, 221–227 (1950).
2. J. C. Y. Koh, Analysis of film boiling on vertical surfaces, *J. Heat Transfer* **84**, 55–62 (1962).
3. E. M. Sparrow and R. C. Cess, The effect of subcooled liquid on laminar film boiling, *J. Heat Transfer* **84**, 149–156 (1962).
4. K. Nishikawa and T. Ito, Two-phase boundary layer treatment of free-convection film boiling, *Int. J. Heat Mass Transfer* **9**, 103–115 (1966).
5. T. B. Dunskus and J. W. Westwater, Effect of trace additives on the heat transfer to boiling isopropanol, *Chem. Engng Prog. Symp. Ser.* **57**, 173–181 (1961).
6. D. E. Kautzky and J. W. Westwater, Film boiling of a mixture on a horizontal plate, *Int. J. Heat Mass Transfer* **10**, 253–256 (1967).
7. P.-L. Yue, Film boiling of binary mixtures, Ph.D. thesis, McGill University, Canada (1971).
8. J. C. Y. Koh, Laminar film condensation of condensible gases and gaseous mixtures on a flat plate, Proceedings of the 4th U.S. National Congress of Applied Mechanics Vol. 2, pp. 1327–1336 (1962).
9. P. W. McFadden and R. J. Grosh, High-flux heat transfer studies: An analytical investigation of laminar film boiling, AEC Research and Development Report ANL-6060 (1959).
10. E. M. Sparrow, Effect of radiation on film boiling heat transfer, *Int. J. Heat Mass Transfer* **7**, 229–238 (1964).
11. N. H. Afgan, Boiling heat transfer and burnout heat flux of ethyl-alcohol–benzene mixtures, Proceedings of the 3rd International Heat Transfer Conference, Vol. 3, pp. 175–185 /1966).

EBULLITION EN FILM DE MELANGES BINAIRES SATURES

Résumé—L'ébullition en film stable d'un mélange binaire saturé est analysée selon la théorie de la couche limite biphasique. On considère à la fois la diffusion et la conduction de chaleur dans la phase liquide. L'analyse montre que de grands accroissements de flux thermique par ébullition en film peuvent être obtenus pour des mélanges à grande volatilité relative. On montre que cet accroissement ne se produit qu'à de petites valeurs de la surchauffe pariétale. Des expériences sur un cylindre horizontal de 7,93 mm dans différents mélanges organiques à la pression atmosphérique montrent un bon accord avec la théorie.

FILMSIEDEN IN GESÄTTIGTEN ZWEISTOFFGEMISCHEN

Zusammenfassung— Stabiles Filmsieden eines Zweistoffgemisches wird an Hand der Zweiphasen-Grenzschichttheorie untersucht. Diffusion und Wärmeleitung in der flüssigen Phase werden berücksichtigt. Die Analyse zeigt, dass, beim Filmsieden grosse Steigerungen des Wärmestroms zu erzielen sind bei Mischungen mit grosser relativer Flüchtigkeit. Man sieht, dass der gesteigerte Wärmeübergang nur bei geringen Wandübertemperaturen auftritt. Versuche an einem horizontalen Zylinder von 7,9 mm Durchmesser in verschiedenen organischen Gemischen bei Atmosphärendruck zeigen gute Übereinstimmung mit der Theorie.

ПЛЕНОЧНОЕ КИНЕНИЕ НАСЫЩЕННЫХ БИНАРНЫХ СМЕМЕЙ

Аннотация—С помощью теории двухфазного пограничного слоя исследуется устойчивое пленочное кипение насыщенной бинарной смеси. При анализе учитывалась как диффузия, так и теплопроводность в жидкой фазе. Показано, что значительное увеличение величины теплового потока при пленочном кипении можно получить смесей с большой относительной летучестью. Показано также, что теплообмен возрастает только при малых значениях перегрева стенки. Экспериментальные значения, полученные при кипении ряда органических смесей на горизонтальном цилиндре диаметром 5/16 дюйма при атмосферном давлении, хорошо согласуются с расчетными.